DeepLoRa: Learning Accurate Path Loss Model for Long Distance Links in LPWAN

Li Liu, Yuguang Yao, Zhichao Cao, Mi Zhang
Michigan State University
{liuli9, yaoyugua, caozc, mizhang}@msu.edu

Abstract—LoRa (<u>Lo</u>ng <u>Ra</u>nge) is an emerging wireless technology that enables long-distance communication and keeps low power consumption. Therefore, LoRa plays a more and more important role in Low-Power Wide-Area Networks (LPWANs), which easily extend many large-scale Internet of Things (IoT) applications in diverse scenarios (e.g., industry, agriculture, city). In lots of environments where various types of land-covers usually exist, it is challenging to precisely predict a LoRa link's path loss. As a result, how to deploy LoRa gateways to ensure reliable coverage and develop precise fingerprint-based localization becomes a difficult issue in practice. In this paper, we propose DeepLoRa, a deep learning-based approach to accurately estimate the path loss of long-distance links in complex environments. Specifically, DeepLoRa relies on remote sensing to automatically recognize land-cover types along a LoRa link. Then, DeepLoRa utilizes Bi-LSTM (Bidirectional Long Short Term Memory) to develop a land-cover aware path loss model. We implement DeepLoRa and use the data gathered from a real LoRaWAN deployment on campus to evaluate its performance extensively in terms of estimation accuracy and model transferability. The results show that DeepLoRa reduces the estimation error to less than 4 dB, which is $2\times$ smaller than state-of-the-art models.

Index Terms—Wireless networks, Low power wide area networks, Attenuation measurement, Propagation losses, Recurrent neural networks.

I. INTRODUCTION

The development of Internet of Things (IoT) has witnessed the explosion of applications, IoT devices, and network size. In many scenarios (e.g., agriculture, industry, city, home, health-care), a large amount of unattended IoT devices are deployed, sending a small volume of data sporadically, which are expected to last for years given limited energy. To simultaneously fulfill all these requirements, extending short-range and low-power wireless techniques with ad-hoc architecture (e.g., wireless sensor networks [1]–[3]) is a common solution in the past decades, which suffers from dramatically increasing deployment and maintenance cost with the increase of network scale. To mitigate this gap, wireless techniques (e.g., LoRa, Sigfox, NB-IoT) for Low-Power Wide Area Networks (LPWANs) have recently emerged. Due to low-cost COTS radio/gateway (e.g., Semtech) and open-source development (e.g., LoRa Alliance), LoRa is gaining popularity in both industry and academy areas [4]–[6].

LoRa physical layer adopts chirp spread spectrum (CSS) modulation [7] to enable data packet reception under low signal-to-noise ratio (SNR) (e.g., -20dBm) while keeping low power consumption (e.g., 400mW transmitting at 20dBm,

5μW in idle mode) as its low duty cycle and narrow bandwidth. The high signal sensitivity enables COTS LoRa radio and gateway to receive the potential weak signals. Hence, LoRa obtains a large link budget [4], [8], [9], which accounts for its high maximum feasible power loss along with the signal propagation between an end node and a gateway. The sufficient link budget can provide reliable coverage spanning from several kilometers to tens of kilometers in various environments (e.g., urban area, rural area).

Though LoRa enables long-distance links, we observe that the communication distance may vary greatly in real-world deployments. When an end node is deployed at different directions of a gateway, the power attenuation of the link, called *path loss*, changes due to different types of land-covers (e.g., tree, buildings, road) along the path. An accurate path loss model is vitally important for LoRaWAN applications. Since path loss correlates to the packet delivery probability of a link [10], if we can accurately predict the path loss associated with a LoRa gateway before it is deployed, we can optimize the LoRaWAN coverage by selecting gateway locations. Moreover, in LoRaWAN, end node localization [11]–[14] relies on the matching of the signal fingerprint (e.g., received signal strength indicator (RSSI)) observed by several gateways. If we can accurately predict path loss without an exhausted site survey, the localization system will be deployed and maintained with low overhead. However, facing the environment diversity in different and large areas of LoRaWAN, it is challenging to develop such an accurate and general path loss model with low overhead [14], [15].

In this paper, we propose DeepLoRa, a learning framework for accurate path loss estimation of long-distance LoRa links. We have two key observations. First, public remote sensing images [14], [15] can be utilized to recognize the fine-grained land-covers distributed along a link. Second, the influence of the land-covers on path loss is actually very complicated. Both the types of land-covers and the order they appear along the link make a difference (Section III-B). Then, we resort to deep learning technique [16]–[18] to model the influence of a specific land-cover distribution on path loss.

Specifically, instead of considering the environment of a LoRa link as a whole, DeepLoRa divides it into an ordered sequence of short links (called *micro link*) with the same length. The detailed land-covers of each micro link are recognized by utilizing remote sensing images. Then we apply a deep neural network with Bidirectional Long-Short-Term-Memory

(Bi-LSTM) units for sequence analysis to learn a path loss model based on the measurements collected from the area of interest. Our Bi-LSTM model inherently models the mapping from land-cover types and order to path loss. When we have trained our model, with only a few extra data collection and model finetuning, the model can be directly transferred to areas with similar land-cover composition.

We implement DeepLoRa and evaluate its performance on the dataset collected from a campus LoRaWAN deployment spanning $6 \times 6km^2$ area in an urban scenario. The dataset involves more than 30,000 packets logged by two gateways sent by 6 mobile end nodes. Experiment results show that DeepLoRa achieves a mean error of 3.56dBm, which is 2× smaller than state-of-the-art models. When we transfer the model from one gateway to the other and finetune it with less than 200 data records, it achieves a mean error of 4.79dBm. Our contributions are summarized as follows:

1) Instead of the physical model, we first propose to utilize deep learning for path loss estimation of long-distance LoRa links across a large area in outdoor scenarios.

2) We empirically study the influence of detailed land-cover sequence on path loss in a real LoRaWAN system. We propose DeepLoRa utilizing adaptive Bi-LSTM model to study the relationship between path loss and the corresponding types and order of land-covers.

3) We implement DeepLoRa and evaluate its performance in real LoRaWAN deployment. The experimental results show that the mean error of DeepLoRa is 2× smaller than state-of-the-art models, and our model can be generalized with low overhead.

The rest of the paper is organized as follows. We introduce the related work in Section II. In Section III, we introduce the problem background and our motivation by illustrating environment modeling challenges. The system design of DeepLoRa is followed in Section IV. Section V and Section VI exhibit the implementation and evaluation, respectively. We conclude our paper in Section VII.

II. RELATED WORK

The characteristics of long-distance wireless links have been empirically studied and theoretically modeled in the past decades. We summarize the existing efforts from the following three aspects.

LoRaWAN field studies: LoSee [10] shows two gateways are needed to ensure the full coverage of the $4.5km^2$ campus. In the deployment of Liando et al. [19], the maximum line-of-sight (LOS) and non-line-of-sight (NLOS) communication distances are approximate 9.08km and 2km when the packet delivery ratio is higher than 70%. Numerous other empirical studies [4], [9], [20]–[24] have been conducted to measure LoRa coverage ranges. The specific range varies with experiment environments. For example, Centenaro et al. [23] observe the range of 2km in an area of high-buildings. Wixted et al. [9] observe coverage of 1km to 20km in the central business district. Different conclusions on LoRa coverage by these empirical studies reveal that path loss increases with

communication distance at different rates in various environments. How to model the impact of the environment on path loss is the focus of designing path loss models. In DeepLoRa, we deploy 2 gateways and 6 mobile end nodes in a campus environment to study the detailed relationship between the land-covers along a LoRa link and the path loss.

Land-cover and environment aware models: A few models are integrating environmental factors to reflect the difference in the rates of path loss increasing. Empirical model Okumura-Hata [25], [26] provides ready-to-use formulas suitable for different environments (e.g., urban, suburban, rural areas). Since those formulas were fitted using data collected in Tokyo, Japan, directly applying this model in new environments with different changing rules of path loss would lead to inaccurate predictions. Bor et al. [4] adopts the well known log-normal shadowing path loss model [27]. Unlike free-space path loss, Bor model uses on-site measurements to estimate the absolute path loss by path loss exponent. These two models only adopt regional environment information for prediction. In this case, the same deployment area would result in the same formulation or path loss exponent, while land-cover compositions of LoRa links are anisotropic. Lacking per-link knowledge of the environment would cause obvious ambiguity in path loss estimation. Demetri et al. [15] and SateLoc [14] adopt remote sensing techniques to analyse the composition of land-covers along LoRa links quantitatively. With the types of land-covers along a LoRa link, Demetri et al. [15] decide which Okumura-Hata formula to use based on the dominating land-cover type. So the effect of land-covers is not directly reflected in the prediction. SateLoc [14] divide the whole link into segments by different land-covers and calculate the overall path loss segment by segment using Bor model with the corresponding path loss exponent, but the result would be of no difference if the order of those segments changes in the link. ALL models mentioned above do not fully utilize the fine-grained environment information. Also, they can not well transfer to new environments due to fixed environment modeling.

Machine learning based models: Some works [28]–[32] use machine learning to model path loss. Oroza et al. [28] adopt random forest algorithm to predict the path loss for American River Hydrologic Observatory wireless links. Zhang et al. [29] use random forest and KNN for evaluating the unmanned aerial vehicle communication channels. Cheng et al. [31] associate the floor plan of a building to RSSI values in each indoor Wi-Fi measurement by Convolutional Neural Networks (CNNs). According to our best knowledge, there is no learning-based approaches for outdoor LoRa path loss estimation yet.

Instead of adopting the physical path loss model, we adopt Recurrent Neural Network based model to depict the complex relationship between the path loss and the types and order of land-cover along the path for more accurate path loss estimation. Furthermore, our model are more transferable because of using less-information-lost raw environment data and highly generalizable RNN models.

TABLE I
THE TYPES OF LAND-COVERS.

NLOS	BUILDING	buidings
	GREENHOUSE	greenhouse structures
	TREES	trees
LOS	Field	farming field or glassland
	SOIL	bare soil
	ROAD	streets,roads and highways
	WATER	lakes and rivers

(a) G_1 (b) G_2

Fig. 1. Path loss vs. distance for different land-cover dominated links regarding to different gateways G_1 and G_2.

III. PROBLEM BACKGROUND AND MOTIVATION

A. LoRa Path Loss Estimation

Generally, actual signal path loss can be calculated by :

$$PL = P^t + G^r + G^t - P^r \quad (1)$$

where P^t is the power fed into the transmitter's antenna, P^r is the Received Signal Strength Indicator(RSSI), G^r and G^t are the power gains at receiver and transmitter sides, respectively. Those terms are in dB(m) units.

In practice, given a received LoRa packet, we can obtain its RSSI and SNR from the gateway, but RSSI is the power combination of LoRa signal and various noises. To eliminate the influence of the noises, we use Expected Signal Power (ESP) [15] as a metric to indicate actual received signal power, which can be derived from the following equation:

$$ESP = RSSI + SNR - 10 \cdot \log_{10}(1 + 10^{0.1SNR}) \quad (2)$$

SNR is in dB unit, the other terms are in dBm units.

Among the models of signal path loss, free-space path loss (FSPL) derived from Friis transmission equation [33] models the path loss in ideal free space scenario which is unobstructed and not affected by multi-path effect, which is given by:

$$FSPL(d) = 10 \log_{10}(d) + 20 \log_{10}(f) - 27.55 \quad (3)$$

where d is the distance between transmitter and receiver whose unit is m, f is the frequency whose unit is MHz.

Researchers adopt various ways to measure the path loss of LoRa links in large open spaces with few obstacles to simulate free-space condition, e.g., using High-altitude weather balloon [15], conduct experiments on beaches/sea with clear sights [19], [20]. The results showed that even in a carefully selected LOS environment, the error between the actual path loss with the path loss estimated by FSPL is still appreciable.

B. The Challenge Of Environment Modeling

As free space conditions can hardly be achieved in reality and FSPL only provides a rough lower bound of the path loss estimation in real LoRa deployment, real-world path loss of LoRa links is susceptible to attenuation caused by the environment.

Environment aware models require acquiring environmental information. Original physical models like Okumura-Hata model and Bor model mainly adopt two approaches: Naked-eye estimations based on experience or on-site measurements, which are usually labor exhausted, especially in long-distance scenarios. Both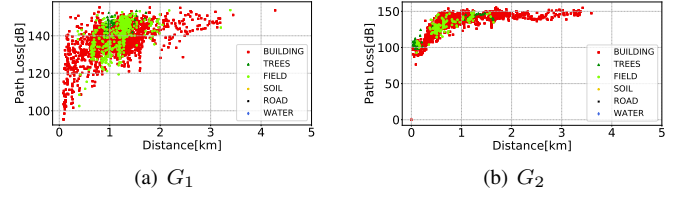 approaches can only provide rough regional environment information. If two LoRa links are in the same deployment area but traverse different kinds of land-covers, they still could be modeled in the same environment using the same formulas/path loss exponents.

We conduct an empirical study based on our LoRaWan system (introduced in IV-D) measurements to find rules according to which different land-covers affect the path loss. All the measurements are collected in the same area. As shown in Figure 1, we color the measured points according to their dominating land-covers along the link. We can see different links have different dominating land-covers (e.g., BUILDING, TREES and FIELD as defined in Table I). Moreover, even under the same distance, the path loss distribution varies for different types of dominating land-covers. BUILDING and FIELD make the path loss more dynamic than other types of land-covers. The result not only shows that different types of land-covers will lead to diverse effects on the path loss, but also emphasize the heterogeneity of LoRa links in the same area. So we need to elaborate per-link environment information for accurate LoRa path loss estimation.

Remote Sensing based Land-cover Recognition. Using remote sensing frees researchers from tedious measurement work while providing rich and fine-grained knowledge of the environment. Literally, remote sensing acquires multi-spectral images of the large-scale area on the earth remotely using air-crafts or satellites equipped with sensors that detect radiation reflected or emitted from target objects. By extracting features from those images and classify them with machine learning models(e.g., Support Vector Machines, Random forest), we can recognize different types of land-covers. In our case, we consider several typical land-covers and divide them into two groups according to whether they may lead to NLOS signal attenuation or not (i.e., LOS transmission) as shown in Table I.

For the two models that utilize remote sensing with physical models, they extend from regional environment modeling to per-link modeling. However, [15] neglects the effect of detailed land-cover types along the link. Because instead of using naked eyes to decide which Okumura-Hata formula to use, [15] utilizes the dominating land-cover type. They choose to use suburban formula if dominating type belongs to LoS category and use urban formula otherwise. Okumura-Hata model actually becomes bottleneck of the whole path loss estimation pipeline. SateLoc [14] ignores the order that different land-covers appear in the link. Because they just divide the whole link into segments and add up the path loss
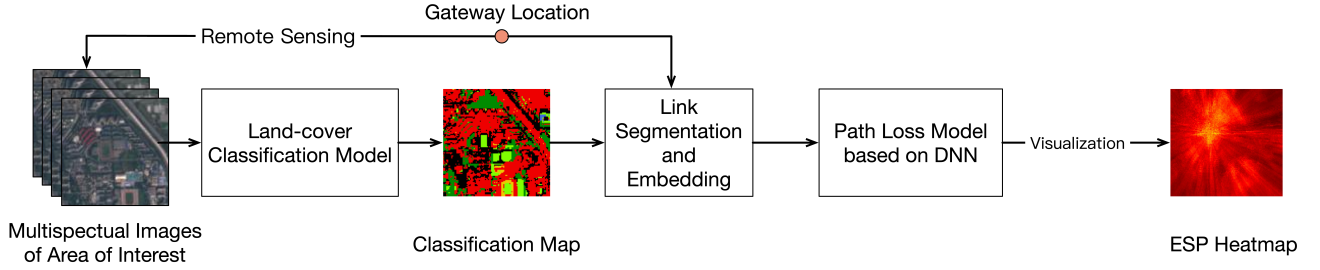
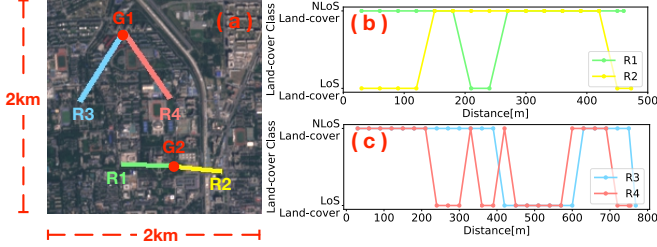Fig. 2. Overview of our system design.

Fig. 3. Four example links in our area of interest.

Link Index	Length[m]	Dominating Land-cover	NLoS Land-cover Percentage	Path Loss[dB]
R_1	46.04	BUILDING	0.61	140.61
R_2	47.27	BUILDING	0.62	114.74
R_3	76.85	BUILDING	0.52	149.34
R_4	75.45	BUILDING	0.52	127.40

for each individual segment, where the order dependency of the segments is actually not used. If we switch the order of the segments in the link, we still get same result.

In Figure 1, we notice that even for the links with the same type of dominating land-covers, their path loss variance is still very significant, especially for G_1. To discuss the problem in detail, we select four links R_1, R_2, R_3 and R_4 from our dataset as shown in Figure 3(a). The properties of those links can be found in Table II. R_1 and R_2, R_3 and R_4 have something in common: 1) their length are nearly the same; 2) the type of dominating land-cover of both links are BUILDING; 3) the percentages of NLoS land-cover of both links are very close. If we adopt models based on land-cover statistics of the link, we should get a very close path loss estimation for each pair of links. However, as shown in our real measurements, the differences between path loss of the two pairs are more than 20dBm, which cannot be ignored.

We plot the detailed types of NLoS and LoS land-covers of these links at a different distance along the path from their end nodes to the gateway in Figure 3(b) and Figure 3(c). We can see that each pair of links show a significant difference in the order that NLoS and LoS land-covers appear. Those links (e.g., R_2 and R_4) with less path loss have less NLoS land-covers near the end node. As other properties of the links remain similar, we believe that not only the types of land-covers affects the path loss, but their order along a link also matters. The reason is that the closer an obstacle to the end node, the more probability the signal can be blocked. Although buildings may block the signal between the end node and the gateway, the limited height of building has less probability to block the signal if it is far away from the end node.

Actually, the LoRa link path loss can be regarded as a result of traversing a sequence of micro-links, the order of the micro-link sequence implicitly influence the path loss. This implicit influence can not be solved by physical path loss models. Based on this understanding, black-box sequence analysis techniques can be used to build the model. Finally, we resort to Recurrent Neural Networks (RNNs), a common architecture of Deep Neural Networks (DNNs), to tackle sequence data and encode the order dependency.

IV. SYSTEM DESIGN

In this section, we first present the overview of DeepLoRa design and several challenging issues, including long link distance, training dataset requirements, and model generalization ability. Then, we illustrate the countermeasures to deal with these challenges. Finally, we introduce a LoRaWAN system deployed on campus in an urban environment to collect the link data.

A. Overview and Design Challenges

In this paper, we propose DeepLoRa, a deep learning-based system aimed at providing accurate path loss estimation by exploiting the types and order of land-covers along a propagation path. Basically, we follow the pattern of combining land-cover recognition with path loss model. Figure 2 shows the overall workflow of our system. DeepLoRa consists of three parts. To start with, given a location where we intend to deploy a LoRa gateway, we generate a land-cover map of the related areas from multi-spectral images through **land-cover classification**. Each pixel in the land-cover map is the class label that represents the true land-cover type in the real map. Then, **Link segmentation and embedding** produces a formalized sequence by segmenting any LoRa link from an end node to the gateway into multiple micro-links of the same length and embedding each micro-link into one element in the sequence based on land-cover map. Moreover, our
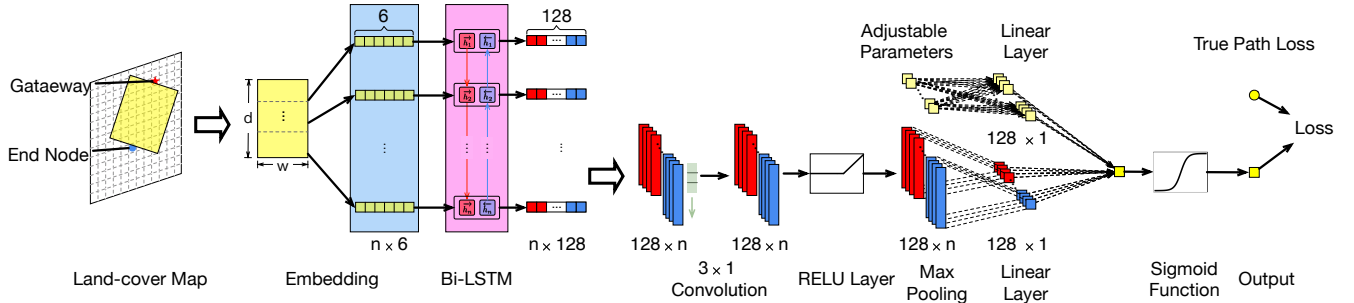
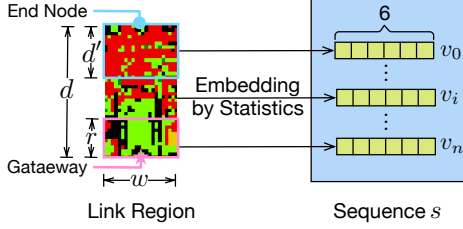Fig. 4. Deep neural network based on Bi-LSTM for path loss prediction.

Fig. 5. Link segment and embedding.

path loss model based on DNN takes the sequences together with experimental specific parameters as input and predicts corresponding path loss such that the ESP received by the gateway can be calculated. Finally, the regional estimation of ESP received by the gateway can be visualized as a heatmap.

It is non-trivial to design such a system, we have 3 major challenges:

1) Deal with long sequences. LoRa links can span extremely long distances(more than 10 kilometers), resulting in quite long sequences. Even if we segment land-cover sequences in coarse granularity, e.g., segment the link into 30m micro-links, we will get a sequence of length 100 for a link of distance 3km. That sequence is equivalent to some paragraphs in machine translation tasks, which is hard to process with more complicated neural architectures. Not to say longer link with finer segmentation granularity. If we segment the link into longer micro-links, the accuracy of granularity will be sacrificed. Therefore, We need to carefully balance the trade-off between sequence length and granularity.

2) Deep learning models require big data. The power of deep models is built on top of sufficient data, while in our scenario collecting data would introduce significant overhead if without an effective method.

3) Costs to transfer to new environments. Model performance in new environments is a common concern of path loss models, including DeepLoRa. As the training cost of DeepLoRa is higher than physical models, this puts forward higher requirements for its transferability between different environments.

In the following sections, we will describe in detail how

DeepLoRa effectively addresses these challenges.

B. Land-cover Classification

Land-cover classification is the first step of DeepLoRa, and it provides us with fine-grained knowledge of the land-cover information traversed by LoRa link. We consider 6 land-cover types in total, as shown in Table I except GREENHOUSE since this class does not present in our experiment area. Actually, it is a per-pixel classification problem. As illustrated by Demetri et al. [15], for each unit area[1] of $10 \times 10m^2$, we extract a feature vector $\mathbf{f}$ including the raw spectral values of corresponding pixel, the Normalized Difference Vegetation Index (NDVI) and the Normalized Difference Water Index (NDWI) from corresponding multi-spectral images. Then, we feed the feature vector to SVMs with Radial Basis Function (RBF) kernel that predicts whether the area belongs to land-cover type $c_k, 0 \le k \le 5$ or not. We can train 6 binary classifiers, each is for one specific land-cover type, and we select the one with the highest confidence score as the final prediction. Overall, we can get the land-cover classification map.

C. Path Loss Estimation

Once we are done with land-cover classification, we can exploit the detailed environment information to design our DNN based path loss model. First, we select a region that can represent the LoRa link. Then, we extract the types of land-covers in the link region as a sequence of micro-environments and further formalize it as the inputs of the DNN learning framework with Bi-LSTM units.

1) Link Segmentation and Embedding: To represent the land-cover composition of a LoRa link, we do not just take a "line" but a rectangular area connecting the end node and the gateway from the land-cover classification map as shown in Figure 4. In our scenario, the direct link is usually NLoS path. The attenuation caused by the environment can be quite complex due to reflection, diffraction, diffusion, and so on, making the "line" hard to be determined. Besides, the misclassification of a few pixels on the line would affect the whole sequence if only one line of pixels is taken into account. Selecting a rectangular area can provide fault tolerance to

---

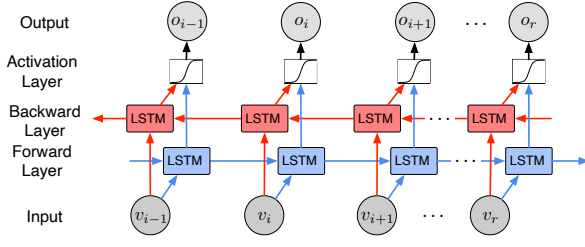[1]10m is the pixel resolution of the multi-spectral images.

Fig. 6. The information flow of Bi-LSTM. $v_{i-1}, v_i, v_{i+1}, v_r$ are vectors in the input sequence, $o_{i-1}, o_i, o_{i+1}, o_r$ are the output hidden states from different frames of Bi-LSTM.

the above concerns. The width of this rectangle needs to be selected according to the experiment and empirical knowledge.

Then, we segment the rectangular area and embed it into the sequence format. Take a closer look at the embedding process in Figure 5. We divide the extracted link of length d and width w into several micro-links of length d' from the end node to the gateway. We can get $n = \lceil d/d' \rceil$ micro rectangles in total. If the remainder $r \neq 0$, we still regard the rest part as a micro-link. The granularity and length of the sequence are determined by d' and have an impact on estimation accuracy. Say that micro-link region $l_i, 0 \leq i < n$ contains $m_k, 0 \leq k \leq 5$ pixels for each land-cover type c_k. Then each micro-link region is embedded into a 1×6 vector v_i by counting the proportion of 6 land-cover types as follows:

$$v_i = [v_i^0, v_i^1, v_i^2, v_i^3, v_i^4, v_i^5]$$
$$v_i^k = m_k / \sum_{j=0}^{5} m_j \tag{4}$$

The rectangle area is now embedded into an ordered sequence $s = [v_0, v_1, ..., v_{n-1}]$. After embedding, we input the sequence to the deep neural network.

2) DNN based Path Loss Model: The architecture of our neural network based path loss model is shown in Figure 4. First, the sequence of the feature vectors is input to Bi-LSTM unit to extract order dependencies. As RNNs can unfold along the time axis (in our case, distance), they enable information flow to traverse from the start of the sequence to the end of the sequence, thus capture the forward dependency and connect the output of the current frame (timestamp, location, etc.) to the previous frame. This capability suits our demand that we want to estimate the path loss at the gateway, which is the last frame in our sequence considering the attenuation from the start of the sequence. One concern is that RNNs are not good at learning long-term dependencies. To avoid the possible vanishing or exploding gradients problem and solve long-term dependencies, we choose to adopt Bidirectional Long Short Term Memory (Bi-LSTM) [34], [35] units instead of original RNNs. Bi-LSTM contains information flow in both directions (e.g., red arrows and blue arrows in Figure 6). This ensures that the land-cover information from both the start and end of the sequence can be captured instead of "forgot" when the length of the sequence is very long.

The output of Bi-LSTM is input into convolution layers to extract local features and context dependency. Rectified Linear Unit (ReLU) layer [36] introduces non-linearity to the model. After max pooling, the output features are down-sampled, and the dimensionality is reduced. Then, we linearly map the features to path loss. To be noted that, while doing linear mapping, we can add extra parameters that have an effect on the path loss to the network. In this way, our network becomes extendable when we have other LoRa link properties, e.g., weather condition, temperature, etc. So that we can quantitatively study new influencing factors in the future. For now, we just input the link distance as well as the height difference of the transmitting antenna and the receiving antenna.

The actual path loss of a LoRa Link has boundaries. It can not be less than 0, it can not exceed the maximum link budget constraint by the maximum transmitting power and end node sensitivity. So we curve our final estimation to a value between 0 and 1 using sigmoid function. In this way, we can control the range of losses for the sake of training convenience. We just need to scale the estimation with the upper boundary to get the predicted path loss. Path loss larger than the upper boundary will be curved to the upper boundary, which indicates failure of packet delivery. The maximum output power of LoRa in different countries/regions can be up to 30dBm, but for most devices, 20dBm is sufficient. LoRa receivers are able to offer a sensitivity of the order of -130dBm [37]. So in our experiments, we take 160dBm as the upper boundary.

Our system design enables 3 levels of generality and can be transferred to a new environment painlessly.
1) We do not manually select features but use a sequence reorganized from real land-cover map with other factors as inputs. Thus, our model can learn a mapping which approximates to the law of signal propagation. This ensures the first level of model generality.
2) When we train our model, we endeavor to select training data covering the links of various distances and land-cover compositions as introduced in Section V-B, then our training dataset spans much room in the full feature space. This ensures the second level of model generality.
3) We adopt a Bi-LSTM based DNN model in our path loss model. Neural networks trained on a large history dataset can be finetuned with a small dataset containing new data to adjust its weights to fit new observations. So when we finetune our model with just a few data from the new environment, it can achieve higher accuracy than the original model in the new environment. This is one advantage over many other machine learning based models since they need to retrain their model with fixed data from scratch and do not promise to get better results. This ensures the third level of model generality.

The first two levels of generality enable fair transferability of the original model while the last level of generality provides a feasible way to enable model fine-tuning. When we have a higher demand for estimation accuracy, it is reasonable to do more on-site measurements for it. We evaluated the generality and tranferability of our model in Section VI-B.
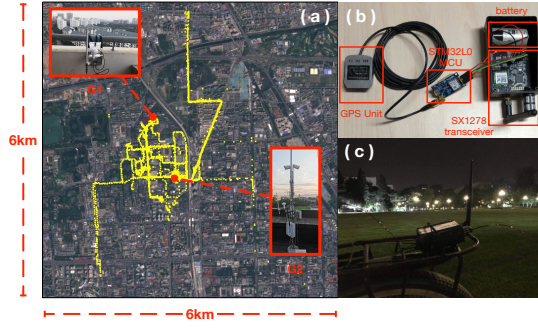
Fig. 7. The overview of the deployment and data samples of our campus LoRaWAN system.

(a) RGB Map   (b) Land-cover Map

Fig. 8. RGB map and land-cover map of the area of interest.

D. Campus LoRaWAN System and Dataset

To enable high-efficiency data collection for empirical study, deep model training, and model performance evaluation, we deploy a LoRaWAN system on campus full of different land-cover types.

Figure 7 shows the overview and hardware of our campus LoRaWAN system. The system is built on the LoRaWAN protocol. In our system, we deployed 2 gateways G_1 and G_2 and 6 mobile end nodes. Each of the gateways is equipped with a MCU, a SX1276 transceiver, and a Raspberry Pi 3 for programming remotely. They are located at the rooftop of two different buildings on campus, as shown in Figure 7(a). Their altitudes are 84m and 68m, respectively. The ground altitude of the campus area is about 52m. Our LoRa end nodes are implemented with a MCU, a SX1278 transceiver and a GPS unit, as shown in Figure 7(b). They are mounted on 5 bicycles and a car, as shown in Figure 7(c). While the bicycles and the car are moving, the LoRa end nodes will send packets to the gateways. All the packets are transmitted with spreading factor SF = 12, bandwidth BW = 125kHz, and coding rate CR = 4/5. The 6 end nodes use channels of 486.3kHz, 486.5kHz, 486.7kHz, 486.9kHz, 487.1kHz and 487.3kHz, respectively. The interval between two adjacent packets is 5s. A packet includes the GPS coordinates, timestamps, and sequence number. The corresponding SNR and RSSI are logged at the gateways. In our system, the sum of P^t, G^r and G^t is 19dB.

We completed deploying the system in Dec, 2018. All the data were collected in the campus or surrounding area from Dec 22, 2018 to Mar 15, 2019. We logged over 30,000 records at the two gateways in total. Via GPS readings, we can calculate the link distance d and the height difference h between an end node's antenna and a gateway's antenna. As shown in Figure 7(a), the measurement locations are along the main roads in or around the campus. The whole region of interest is a $6km \times 6km$ square area where the land-covers include buildings, roads, parking lots, lakes, a river, grassland, trees, and playground. The red points are the locations of our two gateways G_1 and G_2. The yellow points are the locations of all packets transmitted by the moving end nodes.
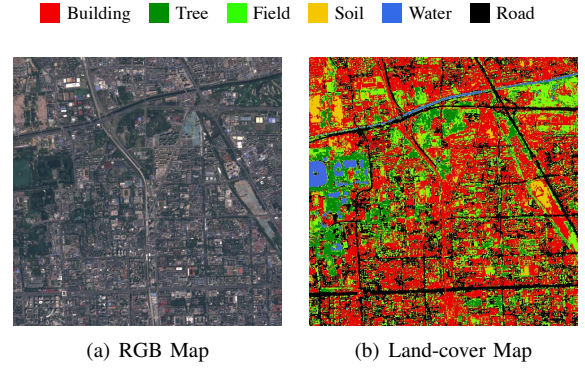
We clean the data and remove redundancy in the way

introduced in Section V-B. Finally, we obtain a dataset that consists of over 4,000 unique records regarding to two gateways. 2,301 records are from G_1 and 1,780 records are from G_2, respectively.

V. IMPLEMENTATION

In this section, we discuss several issues of DeepLoRa implementation.

A. Land-cover Classification

Our land-cover classification shows an overall accuracy of 97.4% for all land-cover types, indicating that we can regard the obtained land-cover map as a reflection of true environment condition. Figure 8(b) shows the generated land-cover map of our area of interest. Different colors indicate different types of land-covers. Most parts of the area are full of buildings. Trees, fields, and roads occupy a large part of the rest area. Water and soil only appear in a few parts of the area.

B. Path Loss Estimation

Our path loss model is based on DNN. We implemented it using Pytorch [38]. We need to use our collected data for model training. While training the model, we have to make sure that two same inputs can only be mapped to the same output. Otherwise our model will be confused. So we clean our data before training. Since our data is continuously collected as the bikes and car move, the locations logged by the GPS unit are continuous on the map. Due to the 10m resolution of multi-spectral images we use, we regard every area of size $10 \times 10m^2$ in reality as a pixel on the map. When we transform the GPS coordinates into coordinates on the map, many locations, in reality, are mapped to the same pixel with different ground-truth path loss. To remove redundancy and get a unique ground truth for each input to the path loss model, we calculate a mean path loss for those measurements with locations that fall into the same pixel.

To train and evaluate our path loss model, we split the dataset into training set and testing set by $9 : 1$. Since our model's principle is sequence processing and the length of a sequence has significant impact on path loss, we separate our data into bins based on their sequence lengths before we

G_{id}	G_1		G_2		all	
	avg	stdd	avg	stdd	avg	stdd
DeepLoRa	3.29	3.12	3.94	3.21	3.56	3.17
INTERSECTION	19.91	7.13	17.55	10.00	18.88	8.58
PATH	20.93	7.68	17.35	10.35	19.36	9.12
Sateloc	12.18	9.21	21.37	15.81	15.61	12.90
Bor	8.70	7.18	12.24	8.83	10.25	8.14
free-space	52.23	6.04	47.52	9.64	50.17	8.16

split the dataset. In this way, we make sure that our training set contains the sequences of diverse lengths, and their distribution in the training set is close to the testing set. Such a balanced training set promises a more general model. However, there is still a gap of the link composition between training sets of two gateways. The two gateways are located at different altitudes, so it remains challenging to apply the model trained for one gateway to a new gateway or new environment directly. We also extract data from training set for two gateways in several proportions, and conduct experiments on model tranferablility between different environments or gateways. We will discuss more about it in Section VI-B.

For the link segmentation and embedding, we select $d = 3$, $w = 7$(represent 30m, 70m respectively) based on model performance in following experiments. We train our model with learning rate $lr = 0.0001$, batch size $train\_bs = 16$, and test the model every 5 epochs.

VI. EVALUATION

In this section, we show DeepLoRa's performance in various environments, and compare DeepLoRa with state-of-the-art models.

A. Overall Performance

We evaluate our model accuracy in comparison with free-space model, Bor model, SateLoc proposed by Liando et al. [19] and two models PATH/INTERSECTION proposed by Demetri et al. [15] on the same testing set by calculating the absolute difference between path loss estimation and ground truth value. The results are shown in Table III.

Among all these models, DeepLoRa achieves the lowest error of less than 4dB for both gateways with the best performance of as low error as 3.29dB, which outperforms those models in comparison by at least 50%. Also, the standard deviation of DeepLoRa is limited to be 3.xdB, the stability of estimation is ensured. We can see that the performance of INTERSECTION/PATH [15] and SateLoc [14] is not as good as claimed, that of original Bor is better instead. The reason is that the path loss exponent of original Bor is obtained by fitting the equation using our training data. In contrast, for SateLoc we use their provided path loss exponents, and INTERSECTION/PATH adopts Okumura-Hata formulations concluded from Tokyo data. The gap between datasets from different environments increases estimation error. DeepLoRa still outperforms the results reported in their original papers.
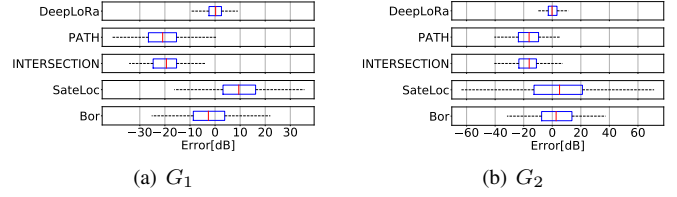

Fig. 9. The distribution of the estimation errors on the full testing set.

G_{id}	$G_1 \rightarrow G_2$		$G_2 \rightarrow G_1$	
	avg (dB)	stdd (dB)	avg (dB)	stdd (dB)
DeepLoRa	9.58	0.76	8.92	6.51
Bor	10.20	9.16	10.00	8.91

We plot the raw estimation errors of these models except free-space model(since its error is too large) on the full testing set in a box plot as Figure 9.

We can see that the raw estimation errors of DeepLoRa are centered around 0dB, which means that it has no tendency to underestimate or overestimate path loss. In contrast, the estimation of other models shows obvious offset towards one side of 0. SateLoc shows more offset from 0 than other approaches proving that the path loss exponents used have a greater gap with the actual rate at which path loss increases with distance. The error distribution of DeepLoRa is way narrower than other models, the magnitude of the largest error is less than 10dB, and the magnitude of 50% errors is less than 5dB. It further proves that DeepLoRa achieves higher estimation accuracy with low variance.

B. Model Generality and Transferability

To compare the transferability of DeepLoRa and other models across environments, we train the model on the training set of one gateway and test it on the testing set of the other. Free-space model, PATH/INTERSECTION do not apply in such scenario (they produce same results as in Table III), we just compare our model with Bor model as in Table IV.

We can see that when DeepLoRa model is trained on G_1 training set and evaluated on G_2 testing set, the average estimation error and the standard deviation is 9.58dB and 0.76dB, which is lower than those of Bor model. We get similar result when we reverse G_1,G_2. This indicates that DeepLoRa guarantees good generality. When we transfer DeepLoRa to a new environment, it still retains satisfactory estimation accuracy.

The above result shows DeepLoRa generality of the first two levels. We also conduct experiments to verify its generality at the third level. Before applying the model directly to the new environment, we finetune the base model with different percentages of training data from the new gateway. Adding 0% of data means using the base model directly without finetuning. The result is given by testing the finetuned model on the testing set of the new gateway, as shown in Figure 11. We can see from the CDF that when test on G_1 data, using 10% G_1
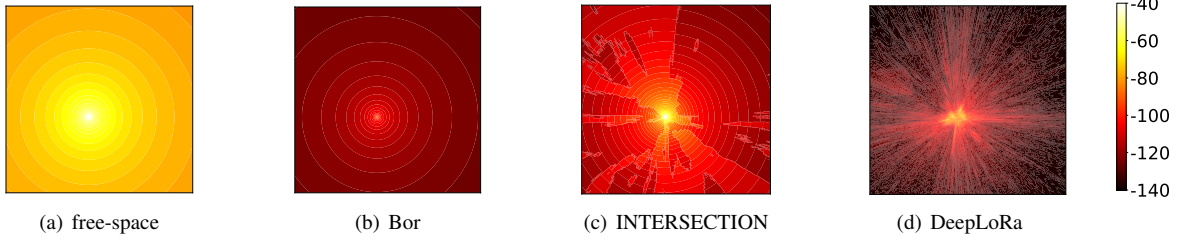
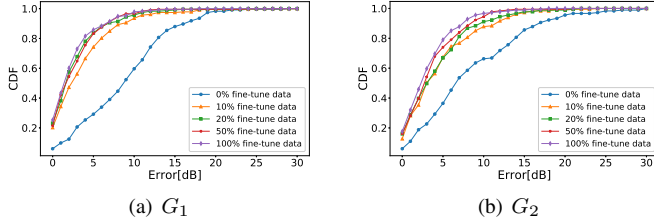Fig. 10. ESP heatmaps of a $6 \times 6km^2$ area with regarding to gateway G_2.

Fig. 11. CDF of absolute estimation error when apply DeepLoRa model in new environment with different amount of finetune data.

G_{id}	$G_1 \to G_2$ (dB)	$G_2 \to G_1$ (dB)
0% finetune data	9.58	8.92
10% finetune data	4.06	5.37
20% finetune data	3.42	4.80
50% finetune data	3.40	4.21
100% finetune data	3.15	3.99

training data for finetuning controls 80% of estimation errors within 7dB. When test on G_2 data, using 10% G_2 training data for finetuning controls 80% of estimation errors within 8.5dB, which approximates the performance when using 100% training data of the new gateway for finetuning (equivalent to train the model from scratch for the new gateway).

In Table V, we report the absolute average estimation error of above experiment. We can see that using 10% of training data to finetune can improve the estimation accuracy up to $2\times$ when compared with no finetuning. And we can see greater improvement when finetuning G_2 model and test on G_1 data. This is because the dataset collected for G_2 is more diverse than that of G_1, resulting in a more general base model. The extra accuracy benefit brought by increasing the amount of finetuning data can be ignored when we already use 20% or more finetune data. In our context, 10% training data is around 200 records, which can be easily collected with our LoRaWan system. Actually, we may not even need 10%, 5% or less would be enough. Based on this result, we suggest first training a base model with large-scale history data obtained from existing real-world deployments and finetuning the base model with a few data collected in the new environment for seek of higher accuracy demand.

C. Generating ESP Heatmap

In order to show the performance of DeepLoRa more intuitively, we do per-link path loss estimation using DeepLoRa for each unit area in the $6\times 6km^2$ area shown in Figure 7. Finally, we draw the ESP heatmap of this area regarding gateway G_2 (G_1's is similar to G_2's). We also draw heatmaps using free-space model, Bor model, and INTERSECTION model for comparison purposes. Figure 10 shows the heatmaps. In these heatmaps we use the same color scale of [-40, -140]dBm for all models, and darker color means lower ESP value (i.e.,

larger path loss). ESP value equal or lower than 140dBm means unable to deliver the packet/no coverage. It is clear that free-space model, and Bor model only provide isotropic path loss estimation with lower accuracy. INTERSECTION model reflects the anisotropy to some extent, but the granularity is not fine enough. When it comes to DeepLoRa, we can see the difference between each link clearly. Many holes of coverage hidden in former heatmaps now show up.

With quantitative experiment results and the visualization for large-scale prediction, we can prove that DeepLoRa is a robust path loss model of high accuracy, it can provide coverage estimation for an area in fine granularity.

VII. CONCLUSION

To conclude, we propose DeepLoRa, a learning framework enabling accurate and general path loss estimation for long-distance wireless links in LPWAN. By deploying a real LoRaWAN system in a campus environment, we empirically study the relationship between the path loss of a link and the land-covers along the link. We have observed that not only the types of land-covers lead to different signal attenuation, but also the order of these land-covers has significant influence. Given an end node position, we utilize remote sensing images to recognize the types of land-covers between the end node and a gateway. Then, we use Bi-LSTM to develop a learning path loss model that captures the influence of both the type and order of these land-covers on the path loss. We implement our learning model and evaluate it based on our dataset. Compared with state-of-the-art physical models, the experimental results show that DeepLoRa achieves more accurate and fine-grained path loss estimation and needs a few transferring training overheads.

REFERENCES

[1] L. Mo, Y. He, Y. Liu, J. Zhao, S.-J. Tang, X.-Y. Li, and G. Dai, "Canopy closure estimates with greenorbs: sustainable sensing in the forest," in *Proceedings of ACM Sensys*, 2009.

[2] X. Mao, X. Miao, Y. He, X.-Y. Li, and Y. Liu, "Citysee: Urban CO_2 monitoring with sensors," in *Proceedings of IEEE INFOCOM*, 2012.

[3] M. Ceriotti, M. Corrà, L. D'Orazio, R. Doriguzzi, D. Facchin, S. Guna, G. P. Jesi, R. L. Cigno, L. Mottola, A. L. Murphy *et al.*, "Is there light at the ends of the tunnel? wireless sensor networks for adaptive lighting in road tunnels," in *Processing of IEEE/ACM IPSN*, 2011.

[4] M. C. Bor, U. Roedig, T. Voigt, and J. M. Alonso, "Do lora low-power wide-area networks scale?" in *Proceedings of ACM MSWiM*, 2016.

[5] J. Haxhibeqiri, E. De Poorter, I. Moerman, and J. Hoebeke, "A survey of lorawan for iot: From technology to application," *Sensors*, vol. 18, no. 11, p. 3995, 2018.

[6] L. Li, J. Ren, and Q. Zhu, "On the application of lora lpwan technology in sailing monitoring system," in *2017 13th Annual Conference on Wireless On-demand Network Systems and Services (WONS)*. IEEE, 2017, pp. 77–80.

[7] B. Reynders and S. Pollin, "Chirp spread spectrum as a modulation technique for long range communication," in *2016 Symposium on Communications and Vehicular Technologies (SCVT)*. IEEE, 2016, pp. 1–5.

[8] L. Vangelista, A. Zanella, and M. Zorzi, "Long-range iot technologies: The dawn of lora™," in *Future access enablers of ubiquitous and intelligent infrastructures*. Springer, 2015, pp. 51–58.

[9] A. J. Wixted, P. Kinnaird, H. Larijani, A. Tait, A. Ahmadinia, and N. Strachan, "Evaluation of lora and lorawan for wireless sensor networks," in *Proceedings of IEEE SENSORS*, 2016.

[10] Y. Yao, Z. Ma, and Z. Cao, "Losee: Long-range shared bike communication system based on lorawan protocol," in *Proceedings of EWSN*, 2019.

[11] K.-H. Lam, C.-C. Cheung, and W.-C. Lee, "Lora-based localization systems for noisy outdoor environment," in *Proceedings of IEEE WiMob*, 2017.

[12] M. Aernouts, R. Berkvens, K. Van Vlaenderen, and M. Weyn, "Sigfox and lorawan datasets for fingerprint localization in large urban and rural areas," *Data*, vol. 3, no. 2, p. 13, 2018.

[13] W. Choi, Y.-S. Chang, Y. Jung, and J. Song, "Low-power lora signal-based outdoor positioning using fingerprint algorithm," *ISPRS International Journal of Geo-Information*, vol. 7, no. 11, p. 440, 2018.

[14] Y. Lin, W. Dong, Y. Gao, and T. Gu, "Sateloc: A virtual fingerprinting approach to outdoor lora localization using satellite images," in *Proceedings of ACM/IEEE IPSN*, 2020.

[15] S. Demetri, M. Zúñiga, G. P. Picco, F. Kuipers, L. Bruzzone, and T. Telkamp, "Automated estimation of link quality for lora: a remote sensing approach," in *Proceedings of ACM/IEEE IPSN*, 2019.

[16] Y. LeCun, Y. Bengio, and G. Hinton, "Deep learning," *nature*, vol. 521, no. 7553, pp. 436–444, 2015.

[17] J. Schmidhuber, "Deep learning in neural networks: An overview," *Neural networks*, vol. 61, pp. 85–117, 2015.

[18] L. Deng, D. Yu *et al.*, "Deep learning: methods and applications," *Foundations and Trends® in Signal Processing*, vol. 7, no. 3–4, pp. 197–387, 2014.

[19] J. C. Liando, A. Gamage, A. W. Tengourtius, and M. Li, "Known and unknown facts of lora: Experiences from a large-scale measurement study," *ACM Transactions on Sensor Networks*, vol. 15, no. 2, p. 16, 2019.

[20] J. Petajajarvi, K. Mikhaylov, A. Roivainen, T. Hanninen, and M. Pettissalo, "On the coverage of lpwans: range evaluation and channel attenuation model for lora technology," in *Proceedings of IEEE ITST*, 2015.

[21] O. Iova, A. Murphy, G. P. Picco, L. Ghiro, D. Molteni, F. Ossi, and F. Cagnacci, "Lora from the city to the mountains: Exploration of hardware and environmental factors," in *Proceedings of EWSN*, 2017.

[22] S. Kartakis, B. D. Choudhary, A. D. Gluhak, L. Lambrinos, and J. A. McCann, "Demystifying low-power wide-area communications for city iot applications," in *Proceedings of ACM WiNTECH*, 2016.

[24] B. Moyer, "Low power wide area: A survey of longer-range iot wireless protocols (2015), retrieved sept. 7, 2015."

[25] Y. Okumura, "Field strength and its variability in vhf and uhf land-mobile radio service," *Rev. Electr. Commun. Lab.*, vol. 16, pp. 825–873, 1968.

[26] M. Hata, "Empirical formula for propagation loss in land mobile radio services," *IEEE Transactions on Vehicular Technology*, vol. 29, no. 3, pp. 317–325, 1980.

[27] T. S. Rappaport *et al.*, *Wireless communications: principles and practice*. Prentice Hall PTR New Jersey, 1996, vol. 2.

[28] C. A. Oroza, Z. Zhang, T. Watteyne, and S. D. Glaser, "A machine-learning-based connectivity model for complex terrain large-scale low-power wireless deployments," *IEEE Transactions on Cognitive Communications and Networking*, vol. 3, no. 4, pp. 576–584, 2017.

[29] Y. Zhang, J. Wen, G. Yang, Z. He, and X. Luo, "Air-to-air path loss prediction based on machine learning methods in urban environments," *Wireless Communications and Mobile Computing*, vol. 2018, 2018.

[30] S. I. Popoola, S. Misra, and A. A. Atayero, "Outdoor path loss predictions based on extreme learning machine," *Wireless Personal Communications*, vol. 99, no. 1, pp. 441–460, 2018.

[31] H. Cheng, H. Lee, and S. Ma, "Cnn-based indoor path loss modeling with reconstruction of input images," in *2018 International Conference on Information and Communication Technology Convergence (ICTC)*. IEEE, 2018, pp. 605–610.

[32] E. Ostlin, H.-J. Zepernick, and H. Suzuki, "Macrocell path-loss prediction using artificial neural networks," *IEEE Transactions on Vehicular Technology*, vol. 59, no. 6, pp. 2735–2747, 2010.

[33] H. T. Friis, "A note on a simple transmission formula," *Proceedings of the IRE*, vol. 34, no. 5, pp. 254–256, 1946.

[34] S. Hochreiter and J. Schmidhuber, "Long short-term memory," *Neural computation*, vol. 9, no. 8, pp. 1735–1780, 1997.

[35] M. Schuster and K. K. Paliwal, "Bidirectional recurrent neural networks," *IEEE Transactions on Signal Processing*, vol. 45, no. 11, pp. 2673–2681, 1997.

[36] X. Glorot, A. Bordes, and Y. Bengio, "Deep sparse rectifier neural networks," in *Proceedings of the fourteenth international conference on artificial intelligence and statistics*, 2011, pp. 315–323.

[37] L. SX1276, "77/78/79 datasheet, rev. 4," *Semtech, March*, 2015.

[38] A. Paszke, S. Gross, F. Massa, A. Lerer, J. Bradbury, G. Chanan, T. Killeen, Z. Lin, N. Gimelshein, L. Antiga, A. Desmaison, A. Kopf, E. Yang, Z. DeVito, M. Raison, A. Tejani, S. Chilamkurthy, B. Steiner, L. Fang, J. Bai, and S. Chintala, "Pytorch: An imperative style, high-performance deep learning library," in *Advances in Neural Information Processing Systems 32*, H. Wallach, H. Larochelle, A. Beygelzimer, F. d'Alché-Buc, E. Fox, and R. Garnett, Eds. Curran Associates, Inc., 2019, pp. 8024–8035. [Online]. Available: http://papers.neurips.cc/paper/9015-pytorch-an-imperative-style-high-performance-deep-learning-library.pdf

[23] M. Centenaro, L. Vangelista, A. Zanella, and M. Zorzi, "Long-range communications in unlicensed bands: The rising stars in the iot and smart city scenarios," *IEEE Wireless Communications*, vol. 23, no. 5, pp. 60–67, 2016.